JAMSTEC Report of Research and Development, Volume 5, March 2007, 9– 19

Wide-angle seismic profiling across the middle Izu-Ogasawara arc for understanding boundary structure between the mature and juvenile arcs - KY0609 cruise -

Narumi Takahashi[1], Takeshi Sato[1], Shuichi Kodaira[1], and Yoshiyuki Kaneda[1]

Abstract We carried out a deep wide-angle seismic experiment using a large airgun array and total 95 ocean bottom seismographs (OBSs) in the middle Izu-Ogasawara arc area, which was conducted by R/V Kaiyo of Japan Agency for Marine-Earth Science and Technology (JAMSTEC) from August 3, 2006 to September 1, 2006 (UTC) named as KY06-09 cruise. The seismic line runs from the Izu-Ogasawara trench to the eastern foot of the Kinan Seamount Chain in the Shikoku basin through the northern tip of the Ogasawara trough, the volcanic front located off south of the Sofugan and the Miocene Nishi-shichito ridge. Most important objective of this cruise is to construct a velocity structure across this area and clarify commonalities and differences by comparison of velocity structures obtained with previous studies in the whole of Izu-Ogasawara arc regions. The key structures are the continuity of the crustal layers of the Ogasawara ridge and trough, and the current active arc obtained by previous KY05-02 and KY05-11 cruises. And the high velocity lower crust with P-wave velocity of over 7.0 km/s is also one of the key structures because it was discovered at the arc-backarc transition zones in the western Izu-Ogasawara arc and the Mariana arc. The seismic signals propagated from an airgun array with a total capacity of 12,000 cu.in. were recorded by not only OBSs but also a 12-channnel streamer towed from stern. In this paper, we introduce the seismic experiment, especially the schedule and examples of OBS and reflection data.

Keywords: Crustal structure, seismic, wide-angle data, OBS, Izu-Ogasawara, backarc rifting

1. Introduction

The Izu-Ogasawara arc is one of best targets to study continental growth because it has andesitic middle crust with P-wave velocity 6 km/s (e.g., Suyehiro et al., 1996), and because the arc growth history, which starts subduction between oceanic crusts, is known (e.g., Hall et al., 1995). The characteristic of SiO_2 content for the Izu-Ogasawara-Mariana oceanic island arc crust indicates basically andesitic and this suggests that the heavy crustal materials included original basaltic crust could be transformed from the crust to the mantle (e.g., Takahashi et al., 2007). This discussion is, however, limited in general characteristic of the Izu-Ogasawara-Mariana arc, and a detailed scenario in response to each arc evolution stage is still unknown. To discuss and understand the crustal growth scenario, a seismic velocity model indicating in situ geological conditions is indispensable.

Some seismic experiments were carried out in the Izu-Ogasawara region and some important commonalities were a thick middle crust with P-wave velocity of 6 km/s, a thick heterogeneous lower crust with relatively high velocity of over 7 km/s and relatively slow one of 6.7-6.8 km/s, and slow mantle velocities of less than typical mantle velocity of 8 km/s (e.g., Suyehiro et al., 1996; Takahashi et al., 1998; Takahashi et al., 2006; Kodaira et al., accepted). A crustal structure along the northern Izu arc indicates that the thickness of the middle crust and the above lower-velocity lower crust contribute to the strong heterogeneity and correlate to chemical composition of igneous rocks collected from outcrops (Kodaira et al., accepted). On the other hand, it is suggested that the southern Izu-Ogasawara arc has thin crust (Yuasa, 1985). The southern Izu-Ogasawara arc is old Eocene arc and includes the Ogasawara trough developed. According to these previous studies, the middle Izu-Ogasawara arc corresponds to a boundary region between the mature northern Izu-Ogasawara arc and the juvenile southern Izu-Ogasawara arc with old Eocene arc.

---

[1] Japan Agency for Marine-Earth Science and Technology

The Ogasawara trough has quite different velocity structure against the northern Izu arc. Two decades ago, a wide-angle seismic survey using ocean bottom seismographs (OBSs) on two seismic lines perpendicular each other, and the velocity structures with no middle crust with P-wave velocity of 6 km/s was obtained (Hino et al., 1989; Katao et al., 1990; Hino et al., 1991). Because some normal faults were found at the both ends of the trough, and because the age of the volcanic rocks collected within the trough is 26-28 Ma (e.g., Abe et al., 1989), it is suggested that the Ogasawara trough is rift zone extended in an old arc before opening of the Shikoku and Parece Vela basins. Recently, it is found by a newly seismic experiment across the Ogasawara ridge old arc that the ridge has middle crust with P-wave velocity of about 6.5 km/s, which is significantly faster than the velocity of current arc middle crust (Takahashi et al., 2006). The distribution of the crust with no middle crust of velocity of 6 km/s is one of key structures to understand crustal growth process.

At adjacent area behind the Sofugan, there is a topographic low, which might correspond to a backarc depression like the Sumisu rift. According to the previous studies (e.g., Corti et al., 2003), a wide rifting may brings anomaly structures known as a core complex by local string crustal thinning and the anomaly might be brought by partial molten region. However, there is no evidence that the topographic low in this experimental area has above partial molten region. If the topographic low may correspond to the active rift advancing crustal differentiation, the heterogeneity of velocity distribution within the crust and the upper mantle might be discovered.

Yuasa (1985) suggested that the Nishinoshima trough is possibly the northern tip of the Parece Vela basin and that this region is located at a boundary between mature northern arc and juvenile southern arc. At the time the proto Izu-Ogasawara arc bended at the current position of the Sofugan (e.g., Yuasa, 1985), the northern tip of the propagated Parece Vela basin (30-15 Ma, Okino et al., 1994) may reach until the Sofugan and the surrounding region. In this case, the high velocity lower crust identified at arc-backarc transition area could be seen around the Sofugan area. In addition, it is known that the Sofugan tectonic line accompanied with the large normal fault bound the northern margin of the Nishinoshima trough. The identification of the normal fault and the mapping may give important information about the tectonics of the middle Izu-Ogasawara region.

The arc-backarc transition area is also one of keys to understand the tectonics and the geological history. According to previous study performed in the Izu-Ogasawara region (e.g, Takahashi et al., 1998), the transition area has high velocity lower crust with P-wave velocity of 7.0-7.5 km/s. In general, a rifting of an initial stage of a backarc opening could accompany with the high velocity region in the boundary zone between the arc and the backarc, and a serpentinization of mantle materials or an underplated gabbroic materials relating to magmatic activity could be candidates of the origin (e.g., Corti et al., 2003). The former and the latter may generally occur at the non-volcanic passive margin and the volcanic passive margin, respectively. In the Izu-Ogasawara region, however, arc magmatic activities with arc evolution after the backarc opening at the eastern margin occurred. The separation of effects by above two processes for the structural variation could be useful for the understanding of the nature.

Here, we mainly set four scientific objectives to be resolved considering above tectonic issues from the seismic velocity model. These four issues are (1) identification and the continuity of the Eocene-Oligocene arc and the past rifting before the Shikoku basin opening, which corresponds to the Ogasawara ridge and the Ogasawara trough, (2) understanding of the current rifting behind the volcanic front by comparison of velocity structures between the current active arc and the topographic low area, (3) identification of the deep normal fault which continues to the Sofugan tectonic line and the high velocity crustal region related to the propagation of the Parece Vela backarc opening, and (4) detection of the high velocity lower crust at the arc-backarc transition zone and the separation of the origins.

To clarify above objectives, we carried out the deep seismic profiling using 95 OBSs, a large airgun array and a 12-channel streamer along a line across the arc in the middle Izu-Ogasawara arc. The only seismic data obtained by this cruise, however, might be difficult to reach final goal. Therefore, we need to consider above scientific issues using not only the result of this cruise but also previous cruise (e.g., Takahashi et al., in Press; Kaiho et al., 2005).

2. Experiment

We carried out a wide-angle seismic profiling using 95 ocean bottom seismographs (OBSs), a large airgun array with capacity of 12,000 cubic inches and a 12-channel analogue streamer in the middle Izu-Ogasawara arc (Figure 1). The period of this cruise using the R/V "Kaiyo" of Japan Agency for Marine-Earth Science and Technology (JAMSTEC) is from August 3 to September 1 (UTC) (Figure 2). We set the main seismic line across the middle Izu-Ogasawara arc near the Sofugan from the Izu-Ogasawara trench to the Kinan seamount chain in the central Shikoku basin. We divided the main line into two parts, which are the most eastern part from the trench

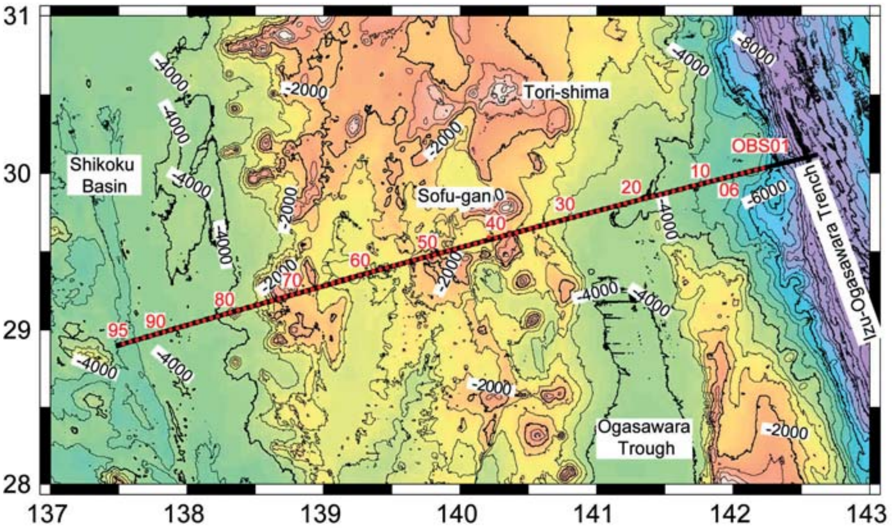

Figure 1: Map of the experimental area. Solid circles indicate OBSs. We shot an airgun array on a thick black line.

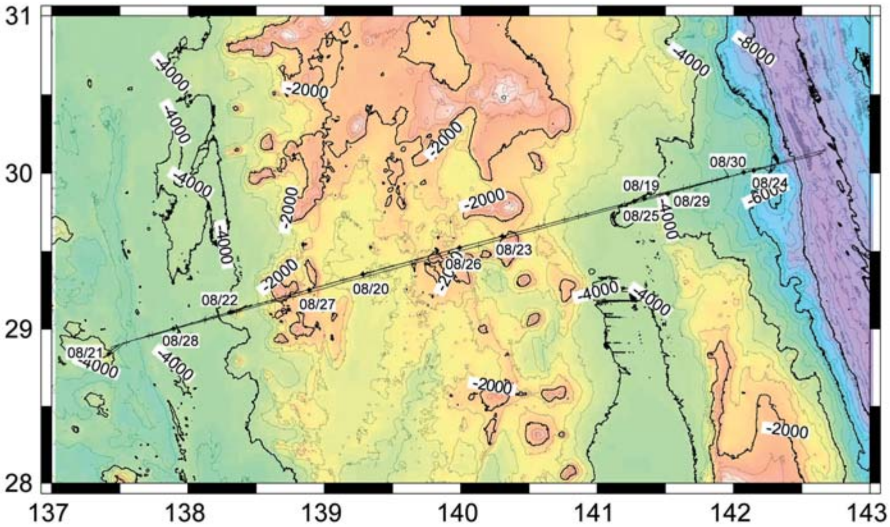

Figure 2: Map for ship's track line. Cross marks indicates ship position of every 6 hours.

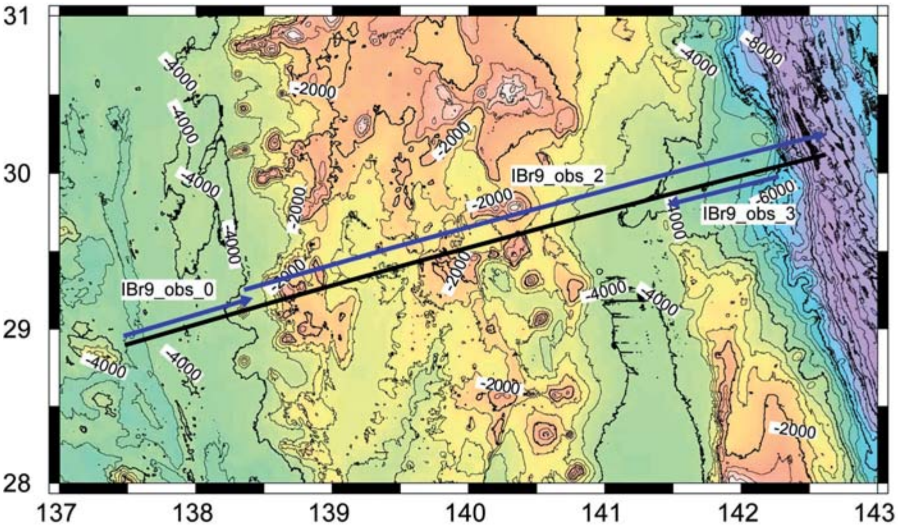

Figure 3: Map of airgun shooting. Blue arrows show a direction of the shooting.

slope break to the eastern forearc basin and the rest of the almost main line considering shortened ship time due to bad weather by typhoon attack season (Figure 3). After departure from Yamashita pier in the Yokohama port on August 3, we had been forced on avoidance in the Tokyo bay by four typhoon attacks for 13 days. We departed from the Tokyo bay on August 17 and deployed 90 OBSs on the main line (Site#6 - Site#95) except the most eastern part from August 18 to 20. We shot the airgun from August 21 to 24 (Lines IBr9_obs_0 and IBr9_obs_2). Then, we recovered 90 OBSs from August 24 to 29. After we deployed 5 OBSs again on the most eastern part on August 29, shot an airgun array on the same day (Line IBr6_obs_3), and then recovered 5 OBSs until August 30. Finally, we arrived at JAMSTEC on September 1. The actual activities are shown in Table 1 and Figure 2.

2.1 Airgun shooting

As described above we shot the airgun array separately for the main line (Lines IBr9_obs_0 and IBr9_obs_2) and the most eastern part (Line IBr9_obs_3). The airgun shooting along the most eastern part after deployment of 5 OBSs (Line IBr9_obs_3) was limited from the Site#16 to Site#1 due to typhoon attacks for five times. The length of the Line IBr9_obs_3 is only 80 km, but we can possibly know the crustal structure until the top of the lower crust according to previous study of the northern Izu arc (Takahashi et al., 1998). The airgun array with a total capacity of 12,000 cubic inches consists of eight airguns (BOLT Technology Corporation, PAR Air Gun Model 1500LL) with 1,500 cubic inches capacity each. The gun array was shot with the shot interval of 200 m and the same timing within 2 msec. The gun depth was 10 m and had kept during airgun shooting. The air pressure sent to the chamber was 2,000 psi. The geometry of the seismic experiment has also kept in the same situation since 2004 (Figure 4) and the details were described by Takahashi et al. (2005). The shot times was measured by a TrueTime system (TrueTime GPS time & frequency receive, MODEL XL-AK) using GPS signals and the accuracy was 1 nsec.

Skyfix and Starfire systems were used as the differential global positioning system (DGPS). The Skyfix system using Naha, Okinawa, Japan station as base station has been adapted as the ship navigation system. The Starfire system has been utilized as the seismic navigation system since 2004. Position data collected by the Skyfix system was used as backup of the seismic navigation system. The accuracy of shot position was about 40 cm.

2.2 Ocean Bottom Seismographs

We deployed 95 OBSs on the seismic line with the interval of 5 km (Figure 1, Table 3). Our seismic group in JAMTSEC has used 5 km as the OBS interval for the wide-angle seismic profiling carried out at the Izu-Ogasawara arc area to simplify comparison among the velocity models with the same resolution obtained along many seismic lines.

All OBSs were equipped with three-component geophones (vertical and two horizontal components perpendicular each other) using gimbal-leveling mechanisms and a hydrophone sensor. Natural frequency of these geophones was 4.5 Hz. The sensitivities of a geophone and hydrophone sensors are shown in Takahashi et al. (2005). Our OBSs and the digital recorder system were originally designed by Kanazawa and Shiobara (1994) and Shinohara et al. (1993). The digital recorder used a 16-bit A/D converter and stored data on digital audiotape or a

Table 1: Activity log during KY06-09 cruise.

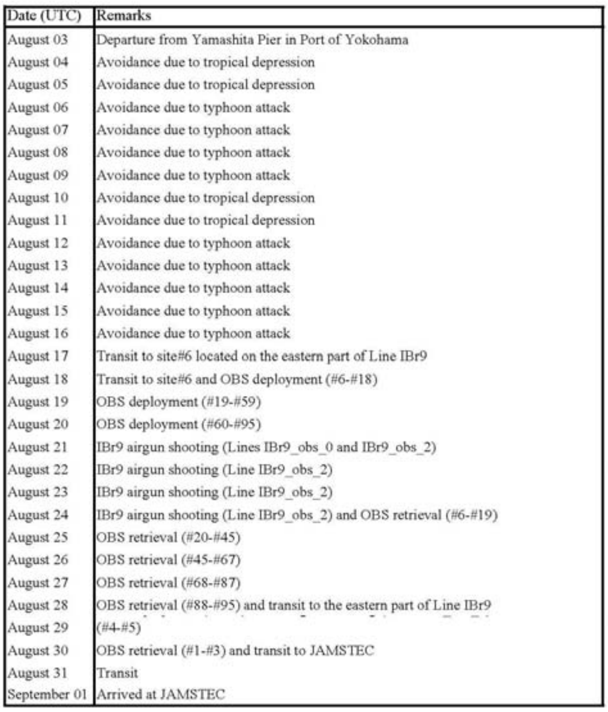

Date (UTC)	Remarks
August 03	Departure from Yamashita Pier in Port of Yokohama
August 04	Avoidance due to tropical depression
August 05	Avoidance due to tropical depression
August 06	Avoidance due to typhoon attack
August 07	Avoidance due to typhoon attack
August 08	Avoidance due to typhoon attack
August 09	Avoidance due to typhoon attack
August 10	Avoidance due to tropical depression
August 11	Avoidance due to tropical depression
August 12	Avoidance due to typhoon attack
August 13	Avoidance due to typhoon attack
August 14	Avoidance due to typhoon attack
August 15	Avoidance due to typhoon attack
August 16	Avoidance due to typhoon attack
August 17	Transit to site#6 located on the eastern part of Line IBr9
August 18	Transit to site#6 and OBS deployment (#6-#18)
August 19	OBS deployment (#19-#59)
August 20	OBS deployment (#60-#95)
August 21	IBr9 airgun shooting (Lines IBr9_obs_0 and IBr9_obs_2)
August 22	IBr9 airgun shooting (Line IBr9_obs_2)
August 23	IBr9 airgun shooting (Line IBr9_obs_2)
August 24	IBr9 airgun shooting (Line IBr9_obs_2) and OBS retrieval (#6-#19)
August 25	OBS retrieval (#20-#45)
August 26	OBS retrieval (#45-#67)
August 27	OBS retrieval (#68-#87)
August 28	OBS retrieval (#88-#95) and transit to the eastern part of Line IBr9
August 29	(#4-#5)
August 30	OBS retrieval (#1-#3) and transit to JAMSTEC
August 31	Transit
September 01	Arrived at JAMSTEC

Table 2: Airgun shooting log.

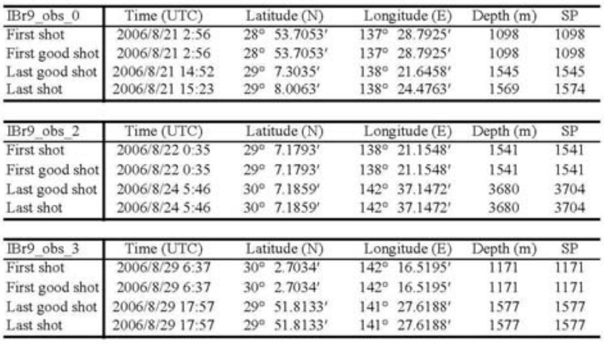

IBr9_obs_0	Time (UTC)	Latitude (N)	Longitude (E)	Depth (m)	SP
First shot	2006/8/21 2:56	28° 53.7053′	137° 28.7925′	1098	1098
First good shot	2006/8/21 2:56	28° 53.7053′	137° 28.7925′	1098	1098
Last good shot	2006/8/21 14:52	29° 7.3035′	138° 21.6458′	1545	1545
Last shot	2006/8/21 15:23	29° 8.0063′	138° 24.4763′	1569	1574

IBr9_obs_2	Time (UTC)	Latitude (N)	Longitude (E)	Depth (m)	SP
First shot	2006/8/22 0:35	29° 7.1793′	138° 21.1548′	1541	1541
First good shot	2006/8/22 0:35	29° 7.1793′	138° 21.1548′	1541	1541
Last good shot	2006/8/24 5:46	30° 7.1859′	142° 37.1472′	3680	3704
Last shot	2006/8/24 5:46	30° 7.1859′	142° 37.1472′	3680	3704

IBr9_obs_3	Time (UTC)	Latitude (N)	Longitude (E)	Depth (m)	SP
First shot	2006/8/29 6:37	30° 2.7034′	142° 16.5195′	1171	1171
First good shot	2006/8/29 6:37	30° 2.7034′	142° 16.5195′	1171	1171
Last good shot	2006/8/29 17:57	29° 51.8133′	141° 27.6188′	1577	1577
Last shot	2006/8/29 17:57	29° 51.8133′	141° 27.6188′	1577	1577

Table 3: OBS information. Each recorder using DAT or hard disk is shown by each abbreviation of D or "H". The "B" and "H" means that makers of the hydrophone sensor are Benthos Inc. and High Tech Inc., respectively.

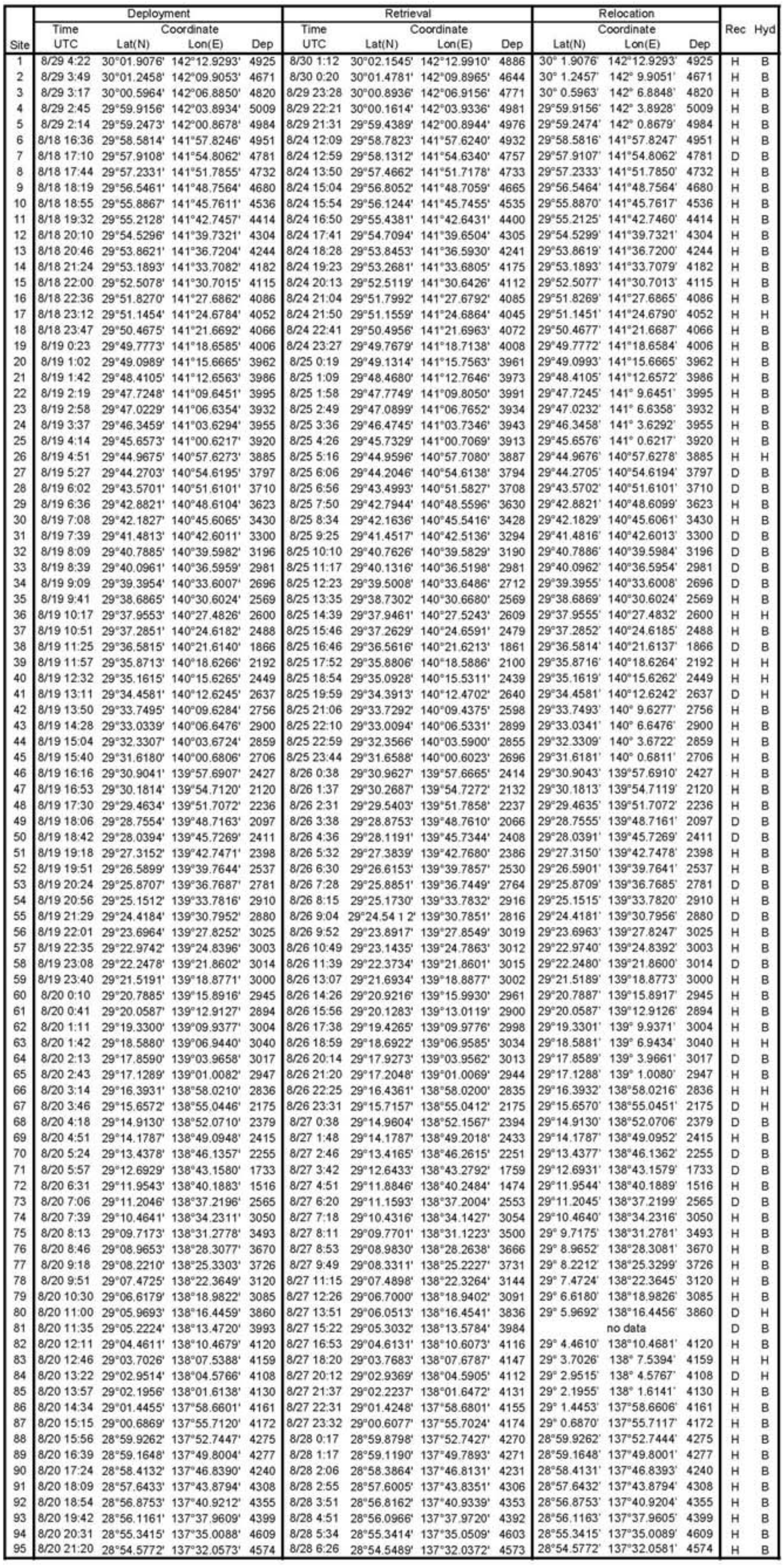

	Deployment				Retrieval				Relocation			Rec	Hyd
	Time	Coordinate			Time	Coordinate			Coordinate				
Site	UTC	Lat(N)	Lon(E)	Dep	UTC	Lat(N)	Lon(E)	Dep	Lat(N)	Lon(E)	Dep		
1	8/29 4:22	30°01.9076'	142°12.9293'	4925	8/30 1:12	30°02.1545'	142°12.9910'	4886	30° 1.9076'	142°12.9293'	4925	H	B
2	8/29 3:49	30°01.2458'	142°09.9053'	4671	8/30 0:20	30°01.4781'	142°09.8965'	4644	30° 1.2457'	142° 9.9051'	4671	H	B
3	8/29 3:17	30°00.5964'	142°06.8850'	4820	8/29 23:28	30°00.8936'	142°06.9156'	4771	30° 0.5963'	142° 6.8848'	4820	H	B
4	8/29 2:45	29°59.9156'	142°03.8934'	5009	8/29 22:21	30°00.1614'	142°03.9336'	4981	29°59.9156'	142° 3.8928'	5009	H	B
5	8/29 2:14	29°59.2473'	142°00.8678'	4984	8/29 21:31	29°59.4389'	142°00.8944'	4976	29°59.2474'	142° 0.8679'	4984	H	B
6	8/18 16:36	29°58.5814'	141°57.8246'	4951	8/24 12:09	29°58.7823'	141°57.6240'	4932	29°58.5816'	141°57.8247'	4951	H	B
7	8/18 17:10	29°57.9108'	141°54.8062'	4781	8/24 12:59	29°58.1312'	141°54.6340'	4757	29°57.9107'	141°54.8062'	4781	D	B
8	8/18 17:44	29°57.2331'	141°51.7855'	4732	8/24 13:50	29°57.4662'	141°51.7178'	4733	29°57.2333'	141°51.7850'	4732	H	B
9	8/18 18:19	29°56.5461'	141°48.7564'	4680	8/24 15:04	29°56.8052'	141°48.7059'	4665	29°56.5464'	141°48.7564'	4680	H	B
10	8/18 18:55	29°55.8867'	141°45.7611'	4536	8/24 15:54	29°56.1244'	141°45.7455'	4535	29°55.8870'	141°45.7617'	4536	H	B
11	8/18 19:32	29°55.2128'	141°42.7457'	4414	8/24 16:50	29°55.4381'	141°42.6431'	4400	29°55.2125'	141°42.7460'	4414	H	B
12	8/18 20:10	29°54.5296'	141°39.7321'	4304	8/24 17:41	29°54.7094'	141°39.6504'	4305	29°54.5299'	141°39.7321'	4304	H	B
13	8/18 20:46	29°53.8621'	141°36.7204'	4244	8/24 18:28	29°53.8453'	141°36.5930'	4241	29°53.8619'	141°36.7200'	4244	H	B
14	8/18 21:24	29°53.1893'	141°33.7082'	4182	8/24 19:23	29°53.2681'	141°33.6805'	4175	29°53.1893'	141°33.7079'	4182	H	B
15	8/18 22:00	29°52.5078'	141°30.7015'	4115	8/24 20:13	29°52.5119'	141°30.6426'	4112	29°52.5077'	141°30.7013'	4115	H	B
16	8/18 22:36	29°51.8270'	141°27.6862'	4086	8/24 21:04	29°51.7992'	141°27.6792'	4085	29°51.8269'	141°27.6865'	4086	H	B
17	8/18 23:12	29°51.1454'	141°24.6784'	4052	8/24 21:50	29°51.1559'	141°24.6864'	4045	29°51.1451'	141°24.6790'	4052	H	H
18	8/18 23:47	29°50.4675'	141°21.6692'	4066	8/24 22:41	29°50.4956'	141°21.6963'	4072	29°50.4677'	141°21.6687'	4066	H	B
19	8/19 0:23	29°49.7773'	141°18.6585'	4006	8/24 23:27	29°49.7679'	141°18.7138'	4008	29°49.7772'	141°18.6584'	4006	H	B
20	8/19 1:02	29°49.0989'	141°15.6665'	3962	8/25 0:19	29°49.1314'	141°15.7563'	3961	29°49.0993'	141°15.6665'	3962	H	B
21	8/19 1:42	29°48.4105'	141°12.6563'	3986	8/25 1:09	29°48.4680'	141°12.7646'	3973	29°48.4105'	141°12.6572'	3986	H	B
22	8/19 2:19	29°47.7248'	141°09.6451'	3995	8/25 1:58	29°47.7749'	141°09.8050'	3991	29°47.7245'	141° 9.6451'	3995	H	B
23	8/19 2:58	29°47.0229'	141°06.6354'	3932	8/25 2:49	29°47.0899'	141°06.7652'	3934	29°47.0232'	141° 6.6358'	3932	H	B
24	8/19 3:37	29°46.3459'	141°03.6294'	3955	8/25 3:36	29°46.4745'	141°03.7346'	3943	29°46.3458'	141° 3.6292'	3955	H	B
25	8/19 4:14	29°45.6573'	141°00.6217'	3920	8/25 4:26	29°45.7329'	141°00.7069'	3913	29°45.6576'	141° 0.6217'	3920	H	B
26	8/19 4:51	29°44.9675'	140°57.6273'	3885	8/25 5:16	29°44.9596'	140°57.7080'	3887	29°44.9676'	140°57.6278'	3885	H	H
27	8/19 5:27	29°44.2703'	140°54.6195'	3797	8/25 6:06	29°44.2046'	140°54.6138'	3794	29°44.2705'	140°54.6194'	3797	D	B
28	8/19 6:02	29°43.5701'	140°51.6101'	3710	8/25 6:56	29°43.4993'	140°51.5827'	3708	29°43.5702'	140°51.6101'	3710	D	B
29	8/19 6:36	29°42.8821'	140°48.6104'	3623	8/25 7:50	29°42.7944'	140°48.5596'	3630	29°42.8821'	140°48.6099'	3623	H	B
30	8/19 7:08	29°42.1827'	140°45.6065'	3430	8/25 8:34	29°42.1636'	140°45.5416'	3428	29°42.1829'	140°45.6061'	3430	H	B
31	8/19 7:39	29°41.4813'	140°42.6011'	3300	8/25 9:25	29°41.4517'	140°42.5136'	3294	29°41.4816'	140°42.6013'	3300	D	B
32	8/19 8:09	29°40.7885'	140°39.5982'	3196	8/25 10:10	29°40.7626'	140°39.5829'	3190	29°40.7886'	140°39.5984'	3196	D	B
33	8/19 8:39	29°40.0961'	140°36.5959'	2981	8/25 11:17	29°40.1316'	140°36.5198'	2981	29°40.0962'	140°36.5954'	2981	D	B
34	8/19 9:09	29°39.3954'	140°33.6007'	2696	8/25 12:23	29°39.5008'	140°33.6486'	2712	29°39.3955'	140°33.6008'	2696	D	B
35	8/19 9:41	29°38.6865'	140°30.6024'	2569	8/25 13:35	29°38.7302'	140°30.6680'	2569	29°38.6869'	140°30.6024'	2569	H	B
36	8/19 10:17	29°37.9553'	140°27.4826'	2600	8/25 14:39	29°37.9461'	140°27.5243'	2609	29°37.9555'	140°27.4832'	2600	H	H
37	8/19 10:51	29°37.2851'	140°24.6182'	2488	8/25 15:46	29°37.2629'	140°24.6591'	2479	29°37.2852'	140°24.6185'	2488	H	B
38	8/19 11:25	29°36.5815'	140°21.6140'	1866	8/25 16:46	29°36.5616'	140°21.6213'	1861	29°36.5814'	140°21.6137'	1866	D	B
39	8/19 11:57	29°35.8713'	140°18.6266'	2192	8/25 17:52	29°35.8806'	140°18.5886'	2100	29°35.8716'	140°18.6264'	2192	H	H
40	8/19 12:32	29°35.1615'	140°15.6265'	2449	8/25 18:54	29°35.0928'	140°15.5311'	2439	29°35.1619'	140°15.6262'	2449	H	H
41	8/19 13:11	29°34.4581'	140°12.6245'	2637	8/25 19:59	29°34.3913'	140°12.4702'	2640	29°34.4581'	140°12.6242'	2637	D	H
42	8/19 13:50	29°33.7495'	140°09.6284'	2756	8/25 21:06	29°33.7292'	140°09.4375'	2598	29°33.7493'	140° 9.6277'	2756	H	B
43	8/19 14:28	29°33.0339'	140°06.6476'	2900	8/25 22:10	29°33.0094'	140°06.5331'	2899	29°33.0341'	140° 6.6476'	2900	H	B
44	8/19 15:04	29°32.3307'	140°03.6724'	2859	8/25 22:59	29°32.3566'	140°03.5900'	2855	29°32.3309'	140° 3.6722'	2859	H	B
45	8/19 15:40	29°31.6180'	140°00.6806'	2706	8/25 23:44	29°31.6588'	140°00.6023'	2696	29°31.6181'	140° 0.6811'	2706	H	B
46	8/19 16:16	29°30.9041'	139°57.6907'	2427	8/26 0:38	29°30.9627'	139°57.6665'	2414	29°30.9043'	139°57.6910'	2427	H	B
47	8/19 16:53	29°30.1814'	139°54.7120'	2120	8/26 1:37	29°30.2687'	139°54.7272'	2132	29°30.1813'	139°54.7119'	2120	H	B
48	8/19 17:30	29°29.4634'	139°51.7072'	2236	8/26 2:31	29°29.5403'	139°51.7858'	2237	29°29.4635'	139°51.7072'	2236	H	B
49	8/19 18:06	29°28.7554'	139°48.7163'	2097	8/26 3:38	29°28.8753'	139°48.7610'	2066	29°28.7555'	139°48.7161'	2097	D	B
50	8/19 18:42	29°28.0394'	139°45.7269'	2411	8/26 4:36	29°28.1191'	139°45.7344'	2408	29°28.0391'	139°45.7269'	2411	D	B
51	8/19 19:18	29°27.3152'	139°42.7471'	2398	8/26 5:32	29°27.3839'	139°42.7680'	2386	29°27.3150'	139°42.7478'	2398	H	B
52	8/19 19:51	29°26.5899'	139°39.7644'	2537	8/26 6:30	29°26.6153'	139°39.7857'	2530	29°26.5901'	139°39.7641'	2537	H	B
53	8/19 20:24	29°25.8707'	139°36.7687'	2781	8/26 7:28	29°25.8851'	139°36.7449'	2764	29°25.8709'	139°36.7685'	2781	D	B
54	8/19 20:56	29°25.1512'	139°33.7816'	2910	8/26 8:15	29°25.1730'	139°33.7832'	2916	29°25.1515'	139°33.7820'	2910	H	B
55	8/19 21:29	29°24.4184'	139°30.7952'	2880	8/26 9:04	29°24.54 1 2'	139°30.7851'	2816	29°24.4181'	139°30.7956'	2880	D	B
56	8/19 22:01	29°23.6964'	139°27.8252'	3025	8/26 9:52	29°23.8917'	139°27.8549'	3019	29°23.6963'	139°27.8247'	3025	H	B
57	8/19 22:35	29°22.9742'	139°24.8396'	3003	8/26 10:49	29°23.1435'	139°24.7863'	3012	29°22.9740'	139°24.8392'	3003	H	B
58	8/19 23:08	29°22.2478'	139°21.8602'	3014	8/26 11:39	29°22.3734'	139°21.8601'	3015	29°22.2480'	139°21.8600'	3014	D	B
59	8/19 23:40	29°21.5191'	139°18.8771'	3000	8/26 13:07	29°21.6934'	139°18.8877'	3002	29°21.5189'	139°18.8773'	3000	H	B
60	8/20 0:10	29°20.7885'	139°15.8916'	2945	8/26 14:26	29°20.9216'	139°15.9930'	2961	29°20.7887'	139°15.8917'	2945	H	B
61	8/20 0:41	29°20.0587'	139°12.9127'	2894	8/26 15:56	29°20.1283'	139°13.0119'	2900	29°20.0587'	139°12.9126'	2894	H	B
62	8/20 1:11	29°19.3300'	139°09.9377'	3004	8/26 17:38	29°19.4265'	139°09.9776'	2998	29°19.3301'	139° 9.9371'	3004	H	B
63	8/20 1:42	29°18.5880'	139°06.9440'	3040	8/26 18:59	29°18.6922'	139°06.9585'	3034	29°18.5881'	139° 6.9434'	3040	H	H
64	8/20 2:13	29°17.8590'	139°03.9658'	3017	8/26 20:14	29°17.9273'	139°03.9562'	3013	29°17.8589'	139° 3.9661'	3017	D	B
65	8/20 2:43	29°17.1289'	139°01.0082'	2947	8/26 21:20	29°17.2048'	139°01.0069'	2944	29°17.1288'	139° 1.0080'	2947	H	B
66	8/20 3:14	29°16.3931'	138°58.0210'	2836	8/26 22:25	29°16.4361'	138°58.0200'	2835	29°16.3932'	138°58.0216'	2836	H	H
67	8/20 3:46	29°15.6572'	138°55.0446'	2175	8/26 23:31	29°15.7157'	138°55.0412'	2175	29°15.6570'	138°55.0451'	2175	D	H
68	8/20 4:18	29°14.9130'	138°52.0710'	2379	8/27 0:38	29°14.9604'	138°52.1567'	2394	29°14.9130'	138°52.0706'	2379	D	B
69	8/20 4:51	29°14.1787'	138°49.0948'	2415	8/27 1:48	29°14.1787'	138°49.2018'	2433	29°14.1787'	138°49.0952'	2415	H	B
70	8/20 5:24	29°13.4378'	138°46.1357'	2255	8/27 2:46	29°13.4165'	138°46.2615'	2251	29°13.4377'	138°46.1362'	2255	D	B
71	8/20 5:57	29°12.6929'	138°43.1580'	1733	8/27 3:42	29°12.6433'	138°43.2792'	1759	29°12.6931'	138°43.1579'	1733	D	B
72	8/20 6:31	29°11.9543'	138°40.1883'	1516	8/27 4:51	29°11.8846'	138°40.2484'	1474	29°11.9544'	138°40.1889'	1516	H	B
73	8/20 7:06	29°11.2046'	138°37.2196'	2565	8/27 6:20	29°11.1593'	138°37.2004'	2553	29°11.2045'	138°37.2199'	2565	D	B
74	8/20 7:39	29°10.4641'	138°34.2311'	3050	8/27 7:18	29°10.4316'	138°34.1427'	3054	29°10.4640'	138°34.2316'	3050	H	B
75	8/20 8:13	29°09.7173'	138°31.2778'	3493	8/27 8:11	29°09.7701'	138°31.1223'	3500	29° 9.7175'	138°31.2781'	3493	H	B
76	8/20 8:46	29°08.9653'	138°28.3077'	3670	8/27 8:53	29°08.9830'	138°28.2638'	3666	29° 8.9652'	138°28.3081'	3670	H	B
77	8/20 9:18	29°08.2210'	138°25.3303'	3726	8/27 9:49	29°08.3311'	138°25.2227'	3731	29° 8.2212'	138°25.3299'	3726	H	B
78	8/20 9:51	29°07.4725'	138°22.3649'	3120	8/27 11:15	29°07.4898'	138°22.3264'	3144	29° 7.4724'	138°22.3645'	3120	H	B
79	8/20 10:30	29°06.6179'	138°18.9822'	3085	8/27 12:26	29°06.7000'	138°18.9402'	3091	29° 6.6180'	138°18.9826'	3085	H	B
80	8/20 11:00	29°05.9693'	138°16.4459'	3860	8/27 13:51	29°06.0513'	138°16.4541'	3836	29° 5.9692'	138°16.4456'	3860	D	H
81	8/20 11:35	29°05.2224'	138°13.4720'	3993	8/27 15:22	29°05.3032'	138°13.5784'	3984	no data			D	B
82	8/20 12:11	29°04.4611'	138°10.4679'	4120	8/27 16:53	29°04.6131'	138°10.6073'	4116	29° 4.4610'	138°10.4681'	4120	H	B
83	8/20 12:46	29°03.7026'	138°07.5388'	4159	8/27 18:20	29°03.7683'	138°07.6787'	4147	29° 3.7026'	138° 7.5394'	4159	H	H
84	8/20 13:22	29°02.9514'	138°04.5766'	4108	8/27 20:12	29°02.9369'	138°04.5905'	4112	29° 2.9515'	138° 4.5767'	4108	D	H
85	8/20 13:57	29°02.1956'	138°01.6138'	4130	8/27 21:37	29°02.2237'	138°01.6472'	4131	29° 2.1955'	138° 1.6141'	4130	H	B
86	8/20 14:34	29°01.4455'	137°58.6601'	4161	8/27 22:31	29°01.4248'	137°58.6801'	4155	29° 1.4453'	137°58.6606'	4161	H	B
87	8/20 15:15	29°00.6869'	137°55.7120'	4172	8/27 23:32	29°00.6077'	137°55.7024'	4174	29° 0.6870'	137°55.7117'	4172	H	B
88	8/20 15:56	28°59.9262'	137°52.7447'	4275	8/28 0:17	28°59.8798'	137°52.7427'	4270	28°59.9262'	137°52.7444'	4275	H	B
89	8/20 16:39	28°59.1648'	137°49.8004'	4277	8/28 1:17	28°59.1190'	137°49.7893'	4271	28°59.1648'	137°49.8001'	4277	H	B
90	8/20 17:24	28°58.4132'	137°46.8390'	4240	8/28 2:06	28°58.3864'	137°46.8131'	4231	28°58.4131'	137°46.8393'	4240	H	B
91	8/20 18:09	28°57.6433'	137°43.8794'	4308	8/28 2:55	28°57.6005'	137°43.8351'	4306	28°57.6432'	137°43.8794'	4308	H	B
92	8/20 18:54	28°56.8753'	137°40.9212'	4355	8/28 3:51	28°56.8162'	137°40.9339'	4353	28°56.8753'	137°40.9204'	4355	H	B
93	8/20 19:42	28°56.1161'	137°37.9609'	4399	8/28 4:51	28°56.0966'	137°37.9720'	4392	28°56.1163'	137°37.9605'	4399	H	B
94	8/20 20:31	28°55.3415'	137°35.0088'	4609	8/28 5:34	28°55.3414'	137°35.0509'	4603	28°55.3415'	137°35.0089'	4609	H	B
95	8/20 21:20	28°54.5772'	137°32.0573'	4574	8/28 6:26	28°54.5489'	137°32.0372'	4573	28°54.5772'	137°32.0581'	4574	H	B

hard disk sampling continuously with original format (Shinohara et al., 1993). The sampling rate is 10 msec. The electronic power for the recorder system of each OBS is supplied by rechargeable lithium-ion batteries. Above geophone sensors with gimbal-leveling mechanism, batteries and a recorder system are installed in 17-inch glass spheres made by Benthos, Inc, USA and Nautilus Marine service GMGH, Germany. To enable easy OBS retrieval after arriving at sea surface, each OBS is attached to a flash light and a beacon with coded signals.

An OBS is deployed by free fall and retrieved by melting releaser composed of stainless steel plates connecting the OBS with a weight when a transponder system receives acoustic signal sent from a vessel. This acoustic communication between the OBS and the vessel was performed using transducers installed on the vessel. Recently, new transponder system has developed by Nippon Marine Enterprises, LTD. and System Giken, LTD in collaboration of JAMSTEC since 2002 (Ito et al., 2002). The new transponder system has ability to enable for continuous sea bottom observation during one year and 512 codes to specify each seabottom equipment. Because we use general over 100 OBSs every year, the many codes enable us to operate OBSs. Positions of OBSs deployed on sea bottom are estimated by traveltimes of direct waves within 5 km from the locations of deployment of each OBS. The accuracy of the estimated OBS position was within 100 m.

After the cruise, we edited the continuous OBS data with length of 70 sec and SEG-Y format. At the same time, the OBS clock was corrected by estimation of time differences between OBS original time and GPS time, which measured just before OBS deployment and just after OBS retrieval.

2.3 Multichannel hydrophone streamer

During airgun shooting, we towed a 12-channel hydrophone streamer to investigate the shallow structures, in particular, a distribution of sediments with low P-wave velocity for the correction to construct a velocity model using OBS data. Moreover, this is useful to detect the fault configurations, which are deep normal faults within the topographic low and the northern end of the Sofugan tectonic line (Figure 4). We used the hydrophone streamer cable (Teledyne Exploration, SDS-55) with a channel interval of 25 m. The lengths of active section and read-in cable from the stern are 300 m and 150 m, respectively, and a distance from the ship stern to the nearest channel is 161 m. The streamer depth was 15 m. Hydrophone sensors with sensitivity of -211.8 dB re V/μPa (20μV/μB) were used and analog signals from 16 sensors in the same channel were stacked before A/D conversion. The frequency characteristic is 5 Hz to 5 kHz. The A/D conversion kit was attached in the recording system, the StrataVisor NX Marine made by Geometrics Inc, and reflection data digitized with 4 msec interval was recorded on DLT tapes with SEG-D 8048 4byte floating point format. System delay, which equals recording start time minus system start time, was 50 msec. The record length was 13.5 sec. A software SPECTRA produced by Concept systems, UK, installed on Linux PC has been used as the seismic navigation system and a GCS90 manufactured by Sercel Inc., USA has been used as the airgun controller system. A flow chart of the recording system using trigger signals controlled by the SPECTRA is exactly the same as the flow of Takahashi et al. (2005) shown in Figure 5. Ship position (reference point of the vessel), shot time (sec), channel position estimated using cable leveler data and length of the read-in cable, water depth obtained by multi-narrow beam data system (Seabeam 2100 systrem), gun position, and shot number are stored with UKOOA P1/90 format.

3. Data

In this chapter, we introduce some representative examples of the seismic data obtained by OBSs and MCS. Vertical components of Site#22 on the forearc

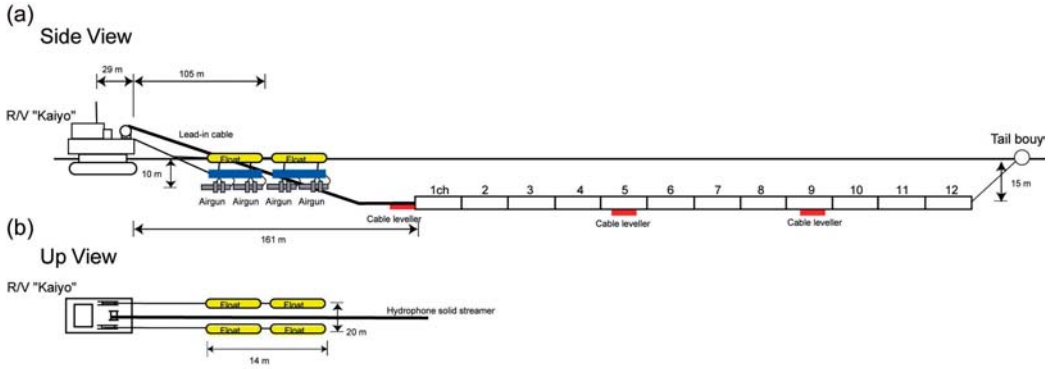

Figure4: Side and up views for geometry of airgun system and the hydrophone streamer.

region, Site#56 near the volcanic front, Site#72 on the Nishi-shichito ridge, Site#86 on the eastern Shikoku basin, and horizontal components of OBS#72 are described in section 3.1. multichannel seismic data (MCS data) are described in section 3.2.

3.1 OBS

We retrieved all OBSs, however, recording system of one OBS had troubles due to a few tears of sea water penetrating into the glass sphere. The quality of most data of available OBSs is basically good and we can trace the first phases on vertical records until 150-200 km distance from each OBS. Reflections also observed almost OBSs. Horizontal records also show good quality despite of poorer S/N ratio than the vertical, and we can see converted S arrivals until about 100 km from the OBS. We describe characteristics of OBS data using vertical record sections of Site#22 (Figure 5), Site#56 (Figure 6), Site#72 (Figure 7) and Site#86 (Figure 8) as follows.

Site#22 was deployed on the forearc region. We can clearly trace first phases to the western offset of 180 km from the OBS (Figure 5) and refraction with weak amplitude continuing to an offset of 300km. The apparent velocities of the refractions with weak amplitude is obviously slower than typical mantle velocity of 8 km/s. This suggested that the mantle velocity beneath the arc region is slow, and is consistent with results conducted along the volcanic front in the northern Izu arc (Kodaira et al., accepted). For inside crust, the apparent velocities of the refractions in the eastern side are 4.3-5.1, 7.1 and 8.1 km/s for offsets of 8-21, 21-34 and 34-46 km, respectively. The apparent velocity becomes small 6.6 km/s at an offset of 46-90 km due to the bathymetric change at the trench slope break and increase to 7.5 km/s at an offset of 94-108 km. In the western side, we can trace them with apparent velocities of 3.3, 4.6, 6.5-6.8 s, 5.6 and 8.1 km/s to offsets of 8-10, 10-15, 37-94, 94-100 and 100-110 km, respectively. The apparent velocity generally has severe change due to rough topography and strong heterogeneity of shallow structure.

OBS#56 was deployed at the western next to the volcanic front. The first phases in the eastern and western sides could be traced to offsets of 120 km and 180 km, respectively (Figure 6).The characteristic of this record is relative slow apparent velocities in both sides. On the eastern side, we can trace first phases with apparent velocities of 3.6, 5.2, 6.7-6.8 and 5.3-6.0 km/s at offsets of 5-10, 10-13, 17-50 and over 50-66 km, respectively. At an offset of over 66 km, the apparent velocity becomes high and over 9 km/s assuming mantle velocity of less than 8 km/s. This suggest that the Moho inclines toward west assuming the first phases identified at offsets of over 66 km to refractions from the mantle. In the western side, the apparent velocities of these phases are 3.5, 5.2, 6.4, 6.7 and 7.2 km/s for offsets of 5-7, 7-11, 11-22 and 35-49 km, respectively. At the eastern offset from 49 km, the apparent velocity has severe change due to the rough topography.

OBS#72 was deployed on the Nishi-shichito ridge. The first phases from distances of about 100 km in both sides can be identified (Figure 7). In the eastern side, we can trace the first phases with apparent velocities of 3.2, 4.4, 6.0 and 7.5 km/s for offsets of 3-11, 11-18, 36-46 and 73-93 km, respectively. Two concave shapes at offsets of 18-36 and 46-73 km are affected topographic high. In the western side, the apparent velocity of the first phases are 2.8, 3.5, 4.1, 5.3, 6.3 and 7.4 km/s for offsets of 6-9, 9-11, 11-15, 15-25, 40-49 and 49-60 km, respectively. At an offset of over 60 km, the refractions from the mantle with apparent velocity of 8.0 km/s can be seen.

OBS#93 was deployed on eastern Shikoku basin. The first phases from the eastern distances of 200 km can be seen (Figure 8). In the eastern side, the apparent velocity changes severe due to rough topography and strong heterogeneity of the shallow structure. At the offsets of 30-60, 80-100 and 100-140 km, clear reflections with relative high amplitude can be seen. The reflections from far side with an offset of over 100 km could be suggested the existence of deep reflectors within the mantle assuming that the crustal structure beneath the OBS is typical oceanic crust.

Figures 9 indicate an example of horizontal records of OBS#72. The first arrivals correspond to the refractions through the crustal and mantle and are also recorded clearly on the vertical component (Figure 7). As after phases, the other phases converted at the basement from P-wave to S-wave are observed at 5-10 sec to an offset of over 100 km. Because the airgun source in the sea water only shot P-wave, we have to trace these converted waves to construct S-wave structure. In the eastern side, we can see them with apparent velocities of 3.2, 3.5, 4.0 and 4.2 km/s at offsets of 10-20, 20-45, 45-80 and 80-95 km, respectively. In the western side, the clear converted S-waves with apparent velocities of 2.5, 3.9, 4.5 and 5.5-5.9 km/s were observed at offsets of 12-14, 18-24, 40-100 and 104-117 km, respectively.

3.2 MCS

The MCS data recorded by a 12-channel hydrophone streamer has enough quality to understand shallow fault configuration. The main part of the MCS profile (Lines IBr9_obs_0 and IBr9_obs_2) and the most eastern part (Line IBr9_obs_3) are shown in Figures 10. Applied tentative flows were a collection of spherical divergence, editing bad quality traces, a time variant filter (3-125 Hz), brute stacking of shot gather with constant velocity of 1500 m/s, a time variant bandpass filter of 20-50 Hz and the auto gain control. Figure 10 indicates the MCS profile and its interpretation. The characteristics of this reflection profile are summarized from west to east as follows.

Beneath the Shikoku basin, we can identify weak reflectors at two-way time of about 9 sec. The reflectors could be interpreted as the Moho assuming the crustal thickness is relatively thin according to previous study (e.g., Suyehiro et al., 1996). For the sedimentary layer, we can see a difference of a character. At the western part from the Kinan escarpment, the thickness of the sedimentary layer is relatively thin. However, the relative thick sedimentary layer composed of two events could be traced from the eastern part of the escarpment.

There are three large topographic highs between the Nishi-shichito ridge and the volcanic front. The sedimen-

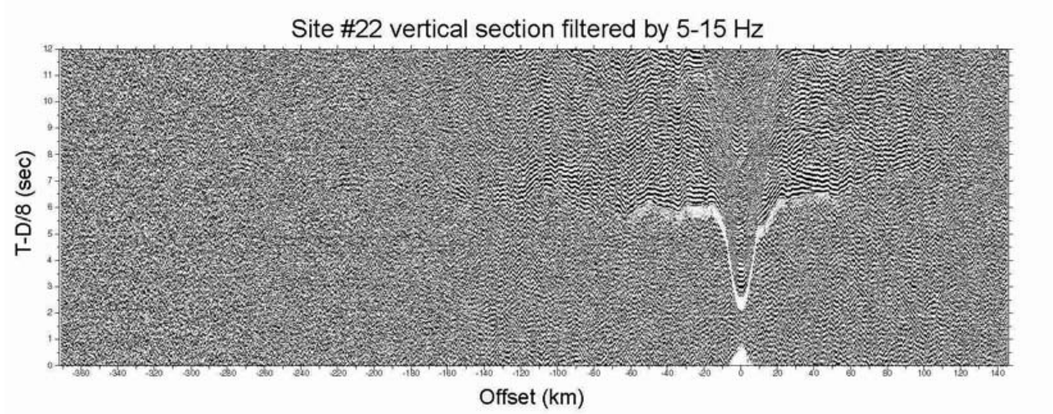

Figure5: Vertical record section recorded by OBS#22. All traces are applied by the bandpass filter with 5-15 Hz. Vertical and horizontal axes are offsets (km) from OBS and traveltimes (sec) reduced by 8 km/s.

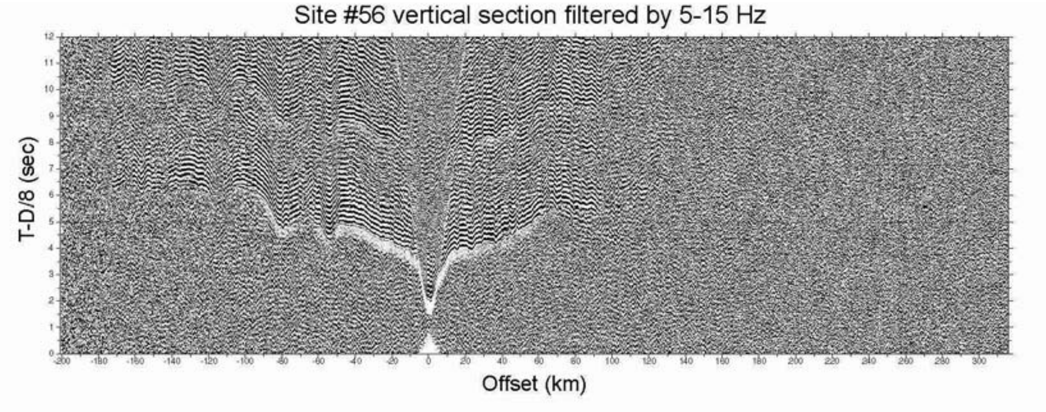

Figure6: Vertical record section recorded by OBS#56. The details are same as for Figure 5.

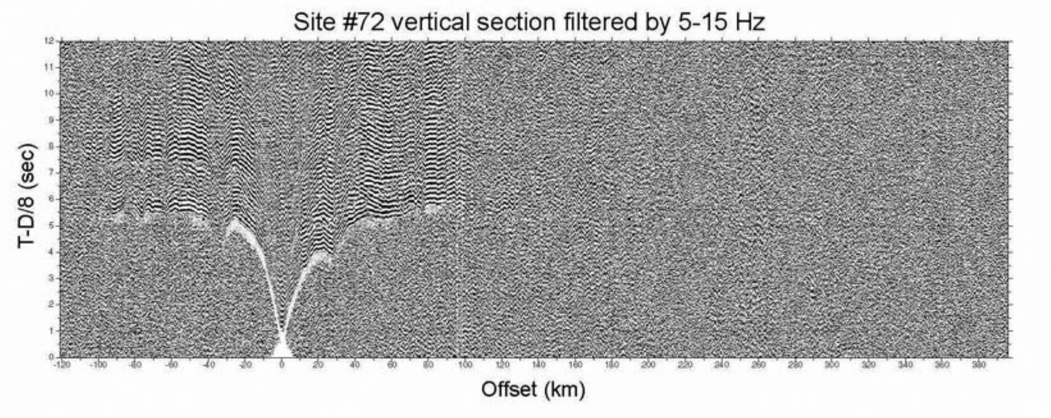

Figure7: Vertical record section recorded by OBS#72. The details are same as for Figure 5.

tary layer exists at only western side and very thin at the eastern basement. In particular, we can see small graben next to the eastern root of the Nishi-shichito ridge. This graben is surrounded by normal faults and this indicates that the active rift develops here. There are no other normal faults in the rift zone. In the northern Izu-Ogasawara ridge, such graben develops behind the volcanic front like the Sumisu rift. It is speculated that the tectonic background in the initial rifting stage of this region might be different with the northern Izu-Ogasawara arc.

In the forearc region, we can see the thick sedimentary layer with the maximum thickness of about 3 sec. The sedimentary layer is composed of three or four events. The thickness becomes thin toward east. These characters are common in the Izu-Ogasawara-Mariana arc. At the trench slope break, there are no clear sedimentary layers. If the Ogasawara ridge continues to this region, the Eocene arc should be located beneath the easternmost

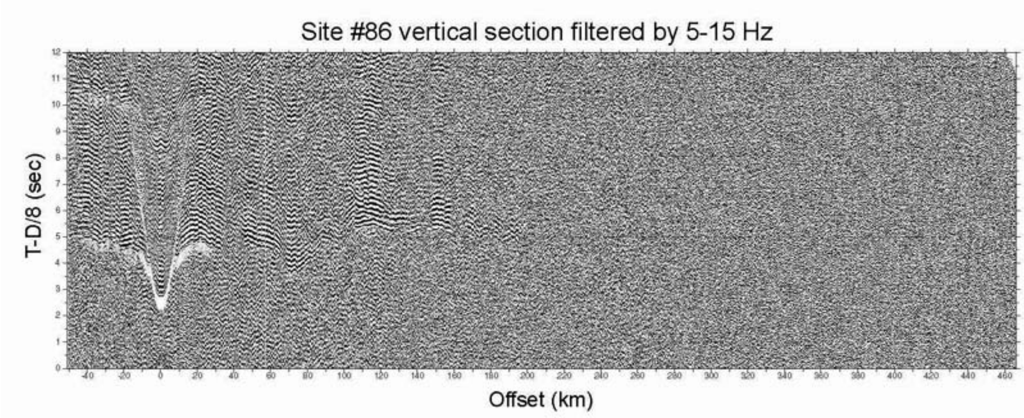

Figure8: Vertical record section recorded by OBS#86 The details are same as for Figure 5.

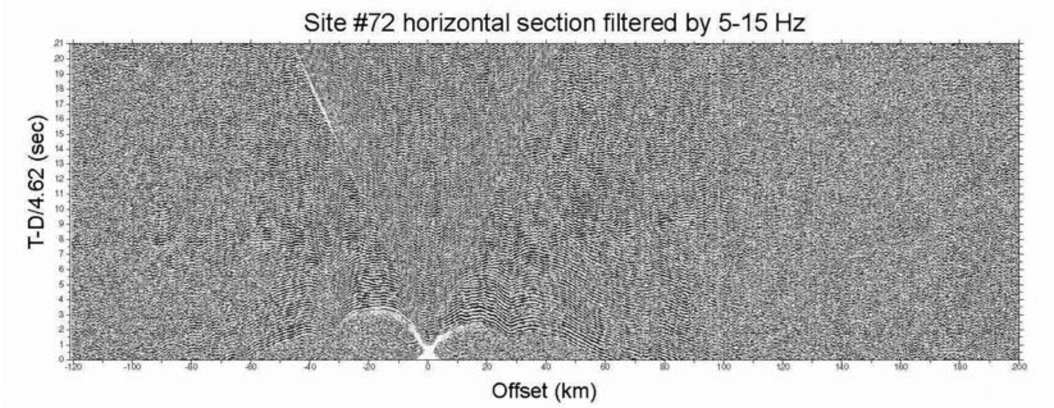

Figure9: Example of horizontal record sections recorded by OBS#72. All traces are filtered by 5-15 Hz. The reduced velocity is 4.62 km/s.

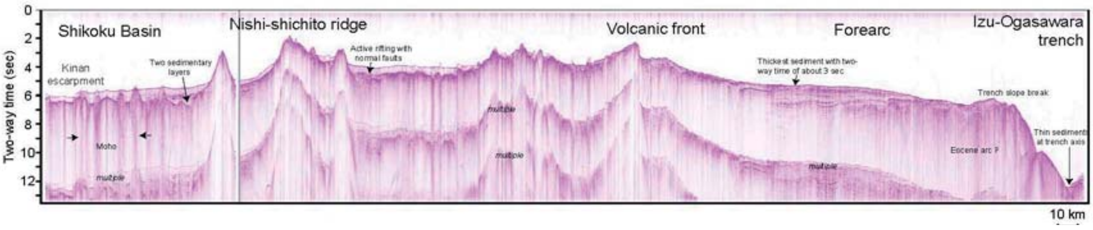

Figure10: MCS profile in stack section.

forearc. The sediments stored on the trench axis is thin and 0.5 sec. It is suggested that much sediments could be subducted beneath the Izu-Ogasawara arc.

4. Summary

We carried out the large active seismic experiment using 95 OBSs, a large airgun array with total capacity of 12,000 cubic inches and a 12-channel hydrophone streamer. Qualities of OBS and MCS data are good to understand the velocity structure and detect the heterogeneity. The OBSs recorded clear phases to the offsets of 150-200 km from each OBS. A part of horizontal components of OBSs are also good and the converted S-waves could be recorded to the offsets of over 100 km. The OBS data suggests that the crustal thickness beneath the arc-backarc transition zone is inferred to be relatively thin considering the offsets from each OBS and the reflection profile. The MCS data indicates the variation of the sedimentary structures and basement. In particularly, the currect active rifting is located the eastern next to the Nishi-shichito ridge not just behind of the volcanic front like the Sumisu rift. This might suggest that the background tectonics of this region is different with that of the northern Izu-Ogasawara arc. The characteristics of the sedimentary layer on the forearc basin are common to those of the northern arc, and the maximum thickness is about 3 sec.

Acknowledgements

We greatly appreciate to following members of KY0609 cruise shipboard party described following, and would not be able to get succession of this seismic experiment without their efforts. We thank S. Miura, M. Yamashita, Y. Kaiho, T. No and K. Takizawa for planning discussion of this cruise and supporting during the cruise.

Marine technicians

Chief Technician	Makoto Ito
Technician	Masato Sugano
Technician	Ikumasa Terada
Technician	Hideki Shibata
Technician	Yuki Ohwatari
Technician	Morifumi Takaesu
Technician	Maki Ito
Technician	Kimiko Serizawa
Technician	Keisuke Onishi
Technician	Hiroyoshi Shimizu
Technician	Chiharu Miwa
Technician	Ayanori Misawa
Technician	Kengo Masui

Crew

Captain	Sadao Ishida
Chief Officer	Shinichi Kusaka
Second Officer	Tadashi Sato
Junior Second Officer	Yoshiyuki Mizui
Third Officer	Kazunori Kamiya
Chief Engineer	Toshihiro Kimura
First Engineer	Chikara Onohara
Second Engineer	Masaya Sumida
Third Engineer	Fumihiko Matsui
Chief Radio Officer	Hideyuki Akama
Second Radio Officer	Kiyotaka Yamashita
Junior Second Radio Officer	Hiroki Ishiwata
Boatswein	Yasuyoshi Kyuki
Able seaman	Kazumi Ogasawara
Able seaman	Katsumi Shimizu
Able seaman	Kazushiro Osako
Able seaman	Hideo Isobe
Able seaman	Tetsuo Shirayama
Sailor	Yoshida Takumi
No.1 Oiler	Kazuaki Nakai
Oiler	Isao Harimoto
Oiler	Yoshinori Kawai
Oiler	Takaatsu Inomoto
Assistant Oiler	Masanori Ueda
Chief Steward	Kyoichi Hirayama
Steward	Shigeto Ariyama
Steward	Isao Matsumoto
Steward	Hiroyuki Yoshizawa
Steward	Hiroyuki Ohba

References

1) Abe, S., H. Tokuyama, S. Kuramoto, K. Suyehiro, A. Nishizawa and H. Kinoshita, Report on DELP 1987 cruises in the Ogasawara area Part II: Seismic reflection studies in the Ogasawara trough, *Bull. Earthq. Rees. Inst., Univ. Tokyo*, 64, 133-147 (1989).

2) Corti, G., M. Bonini, S. Vonticelli, F. Innocenti, P. Manetti and D. Sokoutis, Analogue modeling of continental extension: a review focused on the relations between the patterns of deformation and the presence of magma, *Earth-Sci. Rev.*, 63, 169-247 (2003).

3) Hall, R., Ali, J.R., Anderson, C.D. and Baker S.J., Origin and motion history of the Philippine Sea Plate, *Tectonophysics*, 251, 229-250 (1995)

4) Hino, R., A. Nishizawa, K. Suyehiro, H. Kinoshita, S. Abe, T. Ouchi, A. Kubo, S. Korezawa and S. Nagumo, Report on DELP 1987 cruises in the Ogasawara area Part III: Seismic refraction experiment using airgun-OBSH for fine crustal structure across the Ogasawara trough along east-west track line, *Bull. Earthq. Res. Inst., Univ. Tokyo*, 64, 149-162 (1989).

5) Hino, R., A. Nishizawa, K. Suyehiro and H. Kinoshita, Deep seismic crustal structure beneath the Bonin trough, *Tectonophysics*, 200, 249-266 (1991).

6) Ito, M. and H. Tanaka, The upgrade of ocean-bottom seismograph, *Journal of advanced Marine Science and Technology Society*, in autumn, p2 (2002).

7) Kaiho, Y., N. Takahashi, T. Sato, G. Fujie, S. Kodaira and Y. Kaneda, Wide-angle seismic profiling of oceanic island arc in the southern Izu-Ogasawara arc -KY0502 cruise-, *JAMSTEC Rep. Res. Develop*., 3, 43-52 (2005).

8) IKanazawa,T and H. Shiobara, Newly developed ocean bottom seismometer, *Prog. Abst. Japan Earth and Planetary Science Meeting*, 2, 240 (1994).

9) Katao, H., R. Hino, H. Kinoshita and S. nagumo, Crustal structure of the Bonin trough, *Tectonophysics*, 181, 345-350 (1990).

10) Kodaira, S., T. Sato, N. Takahashi, A. Ito, Y. Tamura, Y. tatsumi and Y. Kaneda, Seismological evidences for variation of continental growth along the Izu Intra-iceanic arc, *J. Geophys. Res*., (accepted)

11) Okino, K., S. Kasuga and Y. Ohara, A new scenario of he Parace Vela basin genesis, *Mar. Geophys. Res*., 20, 21-40 (1998).

12) Shinohara, M., K. Suyehiro, S. Matsuda and K. Ozawa, Digital recording ocean bottom seismometer using portable digital audio tape recorder. *J. Jpn. Soc. Mar. Surv. Tech*., 5, 21-31 (1993). (Japanese with English abstract)

13) Suyehiro, K., N. Takahashi, Y. Ariie, Y. Yokoi, R. Hino, M. Shinohara, T. Kanazawa, N. Hirata, H. Tokuyama, and A. Taira, Continental crust, crustal underplating, and low-Q upper mantle beneath an oceanic island arc, *Science*, 272, 390-392 (1996).

14) Takahashi, N., A. Ito, S. Kodaira and Y. Kaneda, Wide-angle seismic profiling across an active rifted zone in the middle Izu-Ogasawara arc -KY0511 cruise-, *JAMSTEC Rep. Res. Develop*., 4, 27-40, (2006)

15) Takahashi, N., S. Kodaira, S. Klemperer, Y. Tatsumi, Y. Kaneda and K. Suyehiro, Structure and evolution of the Mariana oceanic island arc system, *Geology*, 35, 3, 203-206, (2007)

16) Takahashi, N., K. Suyehiro and M. Shinohara, Implications from the seismic crustal structure of the northern Izu-Ogasawara arc, *The Island arc*, 7, 383-394 (1998).

17) Takahashi, N., S. Kodaira, T. Sato, A. Ito, T. No and Y. Kaneda, Wide-angle seismic profiling of arc-arc collision zone in the northern Izu-Ogasawara arc -KY0408 cruise-, *JAMSTEC Rep. Res. Develop*., 1, 23-36, 2005.

18) Yuasa, M., Sofugan tectonic line, a new tectonic boundary separating northern and southern parts of the Ogasawara (Bonin) arc, northwest Pacific, *Formation of Active ocean margins, eds. Nasu, N. et al*., pp.483-496, 1985.

(Received December 12, 2006)